Atmos. Chem. Phys. Discuss., https://doi.org/10.5194/acp-2018-1333
Manuscript under review for journal Atmos. Chem. Phys.
Discussion started: 10 January 2019

Atmospheric Chemistry and Physics
Discussions

Observation of absorbing aerosols above clouds over the South-East Atlantic Ocean from the geostationary satellite SEVIRI Part 1: Method description and sensitivity

Fanny Peers[1], Peter Francis[2], Cathryn Fox[2], Steven J. Abel[2], Kate Szpek[2], Michael I. Cotterell[1,2], Nicholas W. Davies[1,2], Justin M. Langridge[2], Kerry G. Meyer[3], Steven E. Platnick[3], Jim M. Haywood[1,2]

(1) College of Engineering, Mathematics, and Physical Sciences, University of Exeter, Exeter, UK
(2) Met Office, Exeter, UK
(3) NASA Goddard Space Flight Center, Greenbelt, Maryland, USA

Abstract

High temporal resolution observations from satellites have a great potential for studying the impact of biomass burning aerosols and clouds over the South East Atlantic Ocean (SEAO). This paper presents a method developed to retrieve simultaneously aerosol and cloud properties in aerosol above cloud conditions from the geostationary instrument Meteosat Second Generation/Spinning Enhanced Visible and Infrared Imager (MSG/SEVIRI). The above-cloud Aerosol Optical Thickness (AOT), the Cloud Optical Thickness (COT) and the Cloud droplet Effective Radius (CER) are derived from the spectral contrast and the magnitude of the signal measured in three channels in the visible to shortwave infrared region. The impact of the absorption from atmospheric gases on the satellite signal is corrected by applying transmittances calculated using the water vapour profiles from a Met Office forecast model. The sensitivity analysis shows that a 10% error on the humidity profile leads to an 18.5% bias on the above-cloud AOT, which highlights the importance of an accurate atmospheric correction scheme. *In situ* measurements from the CLARIFY-2017 airborne field campaign are used to constrain the aerosol size distribution and refractive index that is assumed for the aforementioned retrieval algorithm. The sensitivities in the retrieved AOT, COT and CER to the aerosol model assumptions are assessed. Although an uncertainty of 31.2% is observed on the above-cloud AOT, the retrieval of the absorption AOT and both cloud properties is weakly sensitive to the aerosol model assumptions, with biases lower than 7% and 3% respectively. The stability of the retrieval over time is analysed. For observations outside of the backscattering glory region, the time-series of the aerosol and cloud properties are physically consistent, which confirms the ability of the retrieval to monitor the temporal evolution of aerosol above cloud events over the SEAO.

1. Introduction

The South East Atlantic Ocean (SEAO) provides a natural laboratory for analysing the full range of aerosol-cloud-radiation interactions. During the fire season, large amounts of particles from African biomass burning are transported above the semi-permanent deck of stratocumulus covering this oceanic region. As a result, an important contrast is expected in the Direct Radiative Effect (DRE) of aerosols (i.e. the direct impact of aerosol scattering and absorption of radiation). On one hand, the aerosol scattering above the ocean typically increases the local albedo which leads to a negative DRE at the top of the atmosphere. On the other hand, the sign of the DRE above clouds depends on the underlying cloud albedo and the aerosol absorption. Positive instantaneous radiative forcing up to +130W m^{-2} has been observed by satellite instruments over the SEAO (De Graaf et al., 2012; Peers et al., 2015). There are many poorly constrained variables, such as the aerosol and cloud properties, vertical structure of aerosol and clouds (Peers et al., 2016), which result in a large spread in the DRE derived from climate models in this region (Zuidema et al., 2016). In addition, the absorption of radiation by aerosols leads to a modification of the atmospheric stability and consequently on the formation, development and dissipation of clouds, i.e. semi-direct effect. Studies have shown that the overlying African biomass burning aerosols are associated with a cloud thickening (Wilcox, 2010 & 2012). This negative semi-direct effect partly compensates the positive DRE of aerosols above clouds over the SEAO. However, as an aerosol plume moves away from the coast and descends into the boundary layer, the heat due to the aerosol absorption could lead to a reduction of the cloud thickness (Koren et al., 2004). Biomass burning particles may also interact with cloud droplets leading to a modification of the microphysics of the cloud, its lifetime and precipitations (Twomey, 1974; Rosenfeld, 2000). Recent model studies (Gordon et al., 2018; Lu et al., 2018) suggest that the semi-direct and indirect effects of aerosols dominate the DRE over the SEAO, leading to a regional cooling.

Until recently, there has been a relative dearth of observations of biomass burning above clouds as passive sensor retrievals of aerosol and cloud are generally mutually exclusive. In past studies, biases in cloud properties derived from passive shortwave measurements were expected because the impact of aerosol absorption above clouds was not taken into account in the retrievals (Haywood et al., 2004). Over the last decade, techniques have been developed for the observation of Aerosols Above Clouds. POLDER (Polarization measurements from POLarization and Directionality of the Earth's Reflectances) has been used to detect aerosols above clouds and to characterize the aerosol and the cloud layers by exploiting the sensitivity in polarized measurements (Waquet et al., 2013a & 2013b; Peers et al., 2015). In the case of fine mode absorbing aerosols overlying clouds, the absorption Ångström exponent leads to a greater impact on radiances reflected by the clouds at shorter wavelengths than longer ones (De Graaf et al., 2012; Torres et al., 2012). The "colour-ratio" approach has been applied to OMI (Ozone Monitoring Instrument - Torres et al., 2012) and MODIS (Moderate Resolution Imaging Spectroradiometer - Jethva et al., 2013) to simultaneously retrieve the aerosol and the cloud optical thicknesses over the SEAO. Using a similar technique, the MODIS retrieval developed by Meyer et al. (2015) takes advantage of the 6 channels of the instrument from the UV to the Short-Wave Infra-Red (SWIR) to characterize not only the aerosol and cloud optical thicknesses, but also the cloud droplet effective radius. For the first time, these studies have provided large-scale observations of aerosols above clouds in the SEAO. However, these approaches have been applied to satellite instruments on polar orbiting platforms that provide only two observations per day for MODIS (on the Aqua and Terra platforms) and one for OMI and POLDER. The cloud cover over the SEAO is subjected to an important diurnal cycle which

Atmos. Chem. Phys. Discuss., https://doi.org/10.5194/acp-2018-1333
Manuscript under review for journal Atmos. Chem. Phys.
Discussion started: 10 January 2019

Atmospheric Chemistry and Physics
Open Access
Discussions

modulates the DRE of aerosols during the day (Min and Zhang, 2014). Therefore, the study of the SEAO cloud and above-cloud aerosol optical properties requires higher temporal resolution observations from satellite platforms than currently available.

Chang and Christopher (2016) have highlighted the ability of SEVIRI (Spinning Enhanced Visible and Infrared Imager) to identify absorbing aerosols above clouds at high temporal resolution. The instrument is on board the geostationary satellite MSG (Meteosat Second Generation) and provides a full-disc observation every 15 minutes, offering a unique opportunity to monitor the evolution of the cloud cover and to track aerosol plumes over the SEAO. The objective of this two-part paper is to demonstrate the potential of this instrument to retrieve simultaneously aerosol and cloud properties in the case of absorbing aerosols above clouds. In this first contribution, we describe the approach used to derive the above-cloud Aerosol Optical Thickness (AOT), the Cloud Optical Thickness (COT) and the Cloud droplet Effective Radius (CER) and discuss the accuracy of the retrievals. The algorithm, as well as the atmospheric correction scheme and the assumed aerosol model, are presented in Section 2. The sensitivities in the retrieved quantities to the water vapour profile and the aerosol property assumptions are assessed in Section 3. The evaluation of the stability of the retrieval is shown in Section 4 and conclusions are drawn in Section 5. In a second companion paper, we will compare our SEVIRI-based retrievals of cloud and aerosol properties with those from MODIS products (Meyer et al., 2015) and also *in situ* aircraft observations from the CLARIFY-2017 field campaign.

2. Retrieval method

a. Principle

The approach used to retrieve aerosol and cloud properties from satellite spectral radiance measurements relies on the colour-ratio effect (Jethva et al., 2013). The signal backscattered by a liquid cloud is almost spectrally neutral from the UV to the Near Infra-Red (NIR). On the other hand, the absorption from biomass burning aerosols is typically larger at shorter wavelengths. Therefore, the presence of absorbing aerosols above clouds modifies the apparent colour of clouds. This enhancement of the spectral contrast can be detected by any passive remote sensing instrument with two channels with enough separation in the UV/NIR region. The SEVIRI instrument, aboard the MSG satellite (Aminou et al., 1997), has channels centred at 0.64 and 0.81µm. Figure 1 plots the 0.81 µm radiance ($R_{0.81}$) against the ratio of the 0.64 to 0.81 µm radiances ($R_{0.64}/R_{0.81}$), for absorbing aerosols above clouds over an ocean surface for several aerosol and cloud optical thicknesses. Throughout this paper, the radiances refer to the normalized quantity as defined by Herman et al. (2005). The simulations have been performed with the adding-doubling method (De Haan et al., 1987), considering a viewing geometry of 20° for the solar zenith angle, 50° for the viewing zenith angle and 140° for the relative azimuth. The cloud is located between 0 and 1 km and the aerosol layer is between 2 and 3 km. Aerosols have a refractive index of 1.54 - 0.025i and the size distribution follow a lognormal with an effective radius of 0.1µm. The cloud droplets have an effective radius of 10 µm.

Atmos. Chem. Phys. Discuss., https://doi.org/10.5194/acp-2018-1333
Manuscript under review for journal Atmos. Chem. Phys.
Discussion started: 10 January 2019

Atmospheric Chemistry and Physics Discussions
Open Access

Rayleigh scattering has been accounted for but the simulations do not include the absorption from atmospheric gases. A Lambertian surface with an albedo of 0.05 is assumed. For AOT = 0, the radiance ratio is around 1 and is largely invariant as a function of COT. As the AOT increases, the radiance at 0.81µm as well as the radiance ratio decreases, indicating that the attenuation from the aerosol layer is larger at 0.64 µm.

As in the Nakajima and King technique (1990), the sensitivity of the retrieval to the CER is brought by the Short-Wave Infra-Red (SWIR) channel of SEVIRI, centred at 1.64µm. Figure 2 shows the radiances at 0.81 and 1.64 µm for several COT and CER as well as the impact of overlying absorbing aerosols. The simulations without aerosol are plotted in blue and represent the signal typically used by cloud property retrievals that do not include light absorption from overlying aerosols. The orange and red grids are associated with an AOT of 0.5 and 1.5 at 0.55µm. Compared to the no-aerosol case, these grids are shifted towards the upper left, which means that the presence of aerosols decreases the NIR radiance and increases in the SWIR signal. As highlighted by Haywood et al. (2004), not taking into account the aerosol absorption above clouds leads to low biases in both the COT and the CER. These biases depend on the aerosol loading as well as on the brightness of the underlying cloud.

Although the aerosol microphysical properties have some influence on the signal measured by satellites, this kind of approach requires us to assume an aerosol model. Fundamentally, the algorithm developed here aims to retrieve the above-cloud AOT, the COT and the CER from the magnitude and the gradient of the radiances measured by SEVIRI at 0.64, 0.81 and 1.64 µm using a basic Look Up Table (LUT) approach and appropriate assumptions about the aerosol model.

b. Atmospheric correction

The SEVIRI channels chosen for the retrieval are fairly standard in atmospheric science and have been widely used for aerosol and cloud analysis (e.g. Brindley and Ignatov, 2006; Thieuleux, et al. 2005; Watts et al., 1998). However, the SEVIRI bandwidths are much larger than other state-of-the-art instruments such as MODIS, and hence impacted to a greater degree by the absorption from various atmospheric gases. The spectral response functions for the 0.64, 0.81 and 1.64 µm SEVIRI channels are plotted in Figure 3 together with the equivalent MODIS bands. The main absorbing gases in these spectral bands are ozone, water vapour, methane and carbon dioxide; gases which are typically produced and transported within biomass burning plumes (Browell et al., 1996; Koppmann et al., 2005). The contributions of each gas to the atmospheric absorption are also shown in Figure 3 and the two-way transmittances weighted by the spectral response function have been calculated. Although the MODIS bandwidths are narrower than the SEVIRI ones, the weighted transmittances are similar for the 0.64 and 1.64 µm channels. In the NIR, the MODIS central wavelength (0.86 µm) is slightly larger than for SEVIRI (0.81 µm) and the spectral band is only weakly impacted by the humidity, with a weighted transmittance of 0.989. Within the SEVIRI band, water vapour absorption is much higher, with a transmittance of 0.931. As a result, humidity has an impact on the spectral contrast between the VIS and the NIR, and therefore, on the above-cloud AOT retrieval. The atmospheric correction, and especially the water vapour one, is essential to accurately retrieve the aerosol and cloud properties from SEVIRI.

In order to correct the SEVIRI measurements for atmospheric absorption, the transmittances $T_{atm,\lambda}$ are calculated for each spectral band λ from the cloud top height to the top of the atmosphere using the fast-radiative transfer model RTTOV (Matricardi et al., 2004; Hocking et al., 2014). The cloud top height is derived from the Met Office cloud property algorithm which uses the 10.8, 12.0 and 13.4 µm channels of SEVIRI (Francis et al., 2008, Hamann et al., 2014). Water vapour profiles come from the operational forecast configuration of the global Met Office Unified Model (Brown et al., 2012). This forecast is assimilated according to the scheme described by Clayton et al. (2013) that uses humidity data from various sources, including radiosondes and remote sensing sounding data from many meteorological satellites. The forecast is run every 6 hours and the humidity profile used for the atmospheric correction comes from the latest time-appropriate forecast field available. The profiles of the remaining gases - including ozone, carbon dioxide and methane - are those implicitly assumed by the RTTOV calculations (Matricardi, 2008). The radiance measured by SEVIRI $R_{atm,\lambda}$ is finally corrected using:

$$R_{atm,\lambda} = T_{atm,\lambda} R_{\lambda} \quad (1)$$

where R_{λ} is the radiance corrected from the gaseous absorption.

c. Aerosol model

The choice of the aerosol microphysical properties to use for the retrieval is based on *in situ* measurements acquired during the CLARIFY-2017 field campaign. The Facility for Airborne Atmospheric Measurements (FAAM) BAe 146 aircraft was deployed in August-September 2017 operating from Ascension Island, with a main objective of studying biomass burning aerosol interactions with both radiation and clouds over the SEAO. This analysis focuses on flight C050, performed on 04 September, 2017. A profile descent from 7.3 to 1.9 km altitude was performed in order to sample the aerosol layer above clouds. The aerosol dry extinction and absorption were measured with the EXSCALABAR instrument (EXtinction, SCattering and Absorption of Light for AirBorne Aerosol Research), which consists of a series of cavity ring-down and photoacoustic absorption cells operating at different wavelengths (Davies et al., 2018). From these *in situ* measurements, the Single Scattering Albedo (SSA) has been calculated at the instrument wavelengths of 405 and 660 nm. The aerosol size distribution was characterized between 0.05 and 1.50 µm radius using a wing-mounted Passive Cavity Aerosol Spectrometer Probe (PCASP). Before and after the campaign, the bin sizes of the PCASP were calibrated using aerosolized diethyhexyl sebacate and polystyrene latex of known size and refractive index (Rosenberg et al., 2012). Further Mie-scattering theory based calculations are performed in order to determine the bin sizes at the refractive index of the biomass burning aerosol sample. Partial evaporation of water of hydration is expected in the PCASP due to the heating of the probe, which may decrease the aerosol size. However, the sonde dropped during the flight indicates an average relative humidity above clouds of 29.2% with a maximum of

38.6%. According to Magi and Hobbs (2003), the light scattering coefficient of an aged African biomass burning plume only increases by a factor of 1.01 for a relative humidity of 40%. For this reason, the impact of humidity on the PCASP and EXSCALABAR measurements is neglected.

The aerosol properties needed for the SEVIRI retrieval are the size distribution and the complex refractive index. The normalized number size distribution (dN/dlnr) is commonly represented by a combination of lognormal modes:

$$\frac{d\,N}{d\ln\,r} = \sum_i \frac{N_i}{\sqrt{2\pi}} \frac{1}{\ln\sigma_i}\, exp\left[\frac{-(\ln r_i - \ln r)^2}{2(\ln\sigma_i)^2}\right] \quad (2)$$

where N_i, r_i and σ_i are the number fraction, the geometric mean radii and the standard deviation of the mode i, respectively. As in most remote sensing applications, it has been chosen to represent the particle size distribution for the aerosol during CLARIFY-2017 with a fine and a coarse mode contributions. The aerosol model and resulting optical parameters are selected by fitting simultaneously the PCASP measurements (Fig. 4a) and the SSA from EXSCALABAR (Fig. 4b) using Mie theory. The fit of the bimodal distribution has been weighted in order to accurately represent the size range where the SEVIRI retrieval is the most sensitive. The contribution of each PCASP bin to the extinction has been calculated in a similar way to Haywood et al. (2003). The bins corresponding to the 0.15 to 0.25 µm radius range contribute to about 77% of the extinction. Consequently, these bins have been assigned appropriate larger weights during the fitting process of the size distribution. Due to the small fraction of coarse mode aerosols, the standard deviation of this mode σ_{coarse} could not be reliably fitted and has been set to a value of 2.23, which is within the same order of magnitude than the one assumed for absorbing aerosol (~2.12) in the MODIS Dark Target operational algorithm (Levy et al., 2009).

The aerosol model that best represents the PCASP and EXSCALABAR measurements is shown in blue on Figures 4a and 4b. A refractive index of 1.51-0.029i has been obtained, associated with an SSA of 0.85 at 0.55 µm which is within the range of SSA measured during the SAFARI and the DABEX campaigns (Johnson et al., 2008) and on the upper end of the values from Ascension Island reported by Zuidema et al. (2018). Regarding the refractive index, it should be noted that the SSA is not very sensitive to the real part suggesting that the value of 1.51 is not particularly well constrained. However, a real part of 1.51 is consistent with the AERONET retrievals for African biomass burning particles (Sayer et al., 2014) and is adopted here. The best-fit size distribution is characterised by [r_{fine}, σ_{fine}, N_{fine}; r_{coarse}, σ_{coarse}, N_{coarse}] = [0.12µm, 1.42, 0.963; 0.62µm, 2.23, 0.037]. By way of comparison, the 3-mode lognormal distribution obtained for aged biomass burning aerosols during the SAFARI 2000 campaign (Haywood et al., 2003), defined by [r_1, σ_1, N_1; r_2, σ_2, N_2; r_3, σ_3, N_3] = [0.12µm, 1.30, 0.996; 0.26µm, 1.50, 0.0033; 0.80µm, 1.90, 0.0007], is plotted in orange on Figure 4a. The radius associated with the first mode is consistent with the CLARIFY-2017 model. The absence of the second fine mode in this study is compensated by a larger standard deviation for the fine mode. Finally, the radius of the CLARIFY-2017 coarse mode is slightly smaller than the SAFARI one but the coarse mode fractions of the two models are close.

Atmos. Chem. Phys. Discuss., https://doi.org/10.5194/acp-2018-1333
Manuscript under review for journal Atmos. Chem. Phys.
Discussion started: 10 January 2019

d. Algorithm

The algorithm relies on the comparison of the corrected SEVIRI signal at 0.64, 0.81 and 1.64 µm with precomputed radiances. The simulations have been performed using an adding-doubling radiative transfer code (De Haan et al., 1987). The surface is assumed to be Lambertian with an albedo of 0.05 at all wavelengths which is typical of the sea-surface albedo under diffuse radiation conditions. The aerosol and cloud properties assumed for the LUT are summarized in Table 1. The truncation of the cloud droplet phase function has been done using the delta-M method (Wiscombe, 1977) and the TMS correction (Nakajima and Tanaka, 1988) has been applied. The cloud layer is located between 0 and 1 km and the aerosol layer between 2 and 3 km. The sensitivity of the algorithm to the altitudes of the aerosol and cloud layers is expected to be negligible due of the small contribution of the Rayleigh scattering to the signal at the SEVIRI wavelengths. The cloud droplets follow a gamma law distribution characterised by an effective variance of 0.06. When the cloud is optically thin and/or the cloud droplets are too small, it is not possible to separate the contribution to the optical signal arising from aerosols from that of clouds. Therefore, the minimum values for the CER and the COT in the LUT are 4 µm and 3, respectively. This also justifies the assumption of a relatively simple sea-surface reflectance parameterisation as, at COTs exceeding 3, the sea-surface has little impact on the upwelling radiances above clouds. Clouds associated with lower COT and/or CER are rejected. The aerosol model corresponds to the CLARIFY-2017 model mentioned above, assuming the same refractive index at the 3 SEVIRI wavelengths.

The retrieval of the above-cloud AOT, COT and CER is performed simultaneously. The result corresponds to the parameters that minimise the difference ε between the simulated radiances R_{sim} and the corrected satellite signal R_λ:

$$\varepsilon = \sum_{\lambda} \left(\frac{R_\lambda - R_{sim,\lambda}}{R_\lambda} \right)^2 \quad (3)$$

When the simulated signal is not close enough to the satellite measurements (i.e. $\varepsilon > 0.0006$), the result is rejected. The retrieval of the above-cloud AOT is highly uncertain at the cloud edges and for inhomogeneous clouds. In order to remove these results, the products are aggregated onto a 0.1 × 0.1° grid and the standard deviation of the AOT and the CER are calculated. Note that each grid cell represents around 12 SEVIRI observations. The inhomogeneity parameter ρ is defined by the ratio of the standard deviation of a parameter to the average value of this parameter. The results corresponding to a standard deviation of the AOT larger than 0.7 and/or $\rho_{CER} > 0.2$ as well as grid cells associated with less than 9 successful retrievals are rejected.

3. Results and uncertainty analysis

a. Case study

The algorithm has been applied to an event of biomass burning aerosols above clouds captured by SEVIRI on the 28 August 2017 at 10:12 UTC. The RGB composite, the retrieved above-cloud AOT, COT and CER over the SEAO region are shown in Figure 5. The largest AOT are observed off the coast of Angola, with a local average value of 1.0 and a maximum of 1.6 at 550 nm. The AERONET site of Lubango (14.96 ˚S - 13.45 ˚E) measured an average AOT of 0.75 that day with an Ångström exponent of 1.83, indicating the expected domination of fine mode biomass burning aerosols. A gradient of AOT is observed towards the south-west, as we move away from the source as might be expected from a pre-campaign analysis of satellite retrievals (Zuidema et al., 2016). Absorbing aerosols above clouds are also detected in the north-west part of the region. Around Ascension Island (7.98 ˚S - 14.42 ˚W), the above-cloud AOT from SEVIRI is around 0.37 while the AERONET site indicates a value of 0.48 associated with an Ångström exponent of 1.271. This suggests that coarse mode aerosols, such as sea salt within the boundary layer but generally below cloud, are contributing to the total column aerosol load. The cloud properties retrieved are within the range of values typically observed in this region with more than 90 % of the COT lower than 25 and 99 % of the CER between 4 and 20 µm. A good spatial agreement is obtained between the SEVIRI cloud properties and the standard MODIS operational retrieval from the Terra overpasses at 10:00 and 11:30 UTC (Fig. 6). Further comparisons against remote sensing and *in situ* measurements will be presented in a companion paper.

b. Atmospheric correction

The atmospheric transmittances above clouds used to correct the SEVIRI measurements from the gas absorption are calculated based on forecasted water vapour profiles. In order to assess the sensitivity of the retrieval to the atmospheric correction, new transmittances have been calculated for the event studied here, modifying the specific humidity by +/-10%, which can be considered as an upper limit for the error in the forecast model. The aerosol and cloud properties retrieved with the modified atmospheric corrections are aggregated on a $0.1 \times 0.1°$ grid. Figure 7 compares the retrieved aerosol and cloud properties from SEVIRI-measured radiances using the original RH forecast with the perturbed RH (+10% in orange and -10% in blue). The uncertainty on the water vapour content impacts mainly the retrieval of the above-cloud AOT, and then the COT, because of its effect on the radiance ratio. A +10%/-10% bias on the humidity leads to an overestimation/underestimation of the AOT and COT respectively. On average, errors of 18.5%, 5.5% and 2.3% have been calculated for the AOT, COT and CER respectively, based on biases of 10% in the RH forecast. These errors are likely upper estimates because forecast errors in specific humidity are unlikely to reach these values as previously mentioned. However, the differences between forecast model specific humidities and those of simple standard atmosphere climatological values (e.g. those of McClatchey et al., 1972) frequently exceed 10% indicating that accurate retrievals of aerosol and cloud need synergistic retrievals or data assimilated forecasts of specific humidity.

c. Aerosol model

The LUT used for the SEVIRI retrieval uses an assumed aerosol model based on *in situ* measurements from CLARIFY-2017. However, the absorption property and the size of biomass burning particles are expected to vary during the fire season and across the SEAO (e.g. Eck et al., 2003). Here, we analyse the impact of the aerosol assumptions on the retrieved aerosol and cloud properties. New LUTs have been processed, independently modifying each of the following parameters of the CLARIFY-2017 aerosol model: the radius and the standard deviation of the fine mode, the real and the imaginary part of the refractive index. The ranges of the parameter perturbations have been chosen in an attempt to represent the variability of the biomass burning properties over the SEAO. The aerosol properties used for this analysis are summarized in Table 2. The new LUTs have been used to re-process the case study from section 3.a. After aggregating the data on a 0.1 × 0.1° grid, the AOT as well as the Absorption AOT (AAOT), the COT and the CER are compared against those obtained with the standard CLARIFY-2017 aerosol model.

Figure 8 and 9 show the impact of a variation of +/-0.01 µm on the fine mode radius and +/-0.1 on the fine mode standard deviation. For each aerosol and cloud property, a linear relationship is observed between the retrieval using the standard CLARIFY-2017 aerosol model and the modified one. The aerosol size distribution has little influence on the retrieved cloud properties. On average, the modification of the fine mode standard deviation leads to a difference of 2.2% on the COT and 1.0% the CER. The effect associated with a change in the fine mode radius is even lower than 1%. As expected, the above-cloud AOT is more sensitive to the aerosol size distribution used for the inversion and differences up to 11.8% have been observed when the fine mode standard deviation is decreased by 0.1. However, the retrieval of the AOT is based on the detection of the aerosol absorption of the light reflected by the clouds. Therefore, the impact of an error on the aerosol size distribution on the AAOT retrieval is reduced to 5.4% for the standard deviation and 1.4% for the fine mode radius.

To assess the impact of the assumed aerosol refractive index on the retrieved aerosol and cloud properties of interest, variations of +/-0.02 and +/-0.008 have been applied to the real and imaginary parts of the refractive index, respectively. Figure 10 and 11 compare the retrieved aerosol and cloud properties from SEVIRI radiance data for the CLARIFY-2017 aerosol model with those retrieved when the aerosol refractive index parameters are perturbed. The influence of refractive index is similar to the one of the modified aerosol size distribution in that differences of <1% are observed in both COT and CER and a larger impact is found on the AOT with differences up to 39% where the imaginary refractive index is decreased by 0.008. The magnitude of the impact on the AOT is correlated to the difference of SSA between the CLARIFY-2017 and the perturbed aerosol model. Therefore, the retrieval of the AAOT is also less sensitive to the assumption on the aerosol refractive index, with an impact lower than 6.5%.

In order to evaluate the uncertainty u_{aer} of the retrieved aerosol and cloud properties due to the aerosol model assumptions, we combined the uncertainty u_i from the above sensitivity studies using:

$$u_{aer} = \sqrt{u_{r_{fine}}^2 + u_{\sigma_{fine}}^2 + u_{n_{real}}^2 + u_{n_{im}}^2} \quad (4)$$

The uncertainty has been estimated at 31.2% on the AOT, 2.3% on the COT and 1.2 % on the CER. Owing to the sensitivity of the retrieval to the aerosol absorption above clouds, a 6.1% uncertainty has been obtained on the AAOT, which is, together with the cloud albedo, the main parameter for the estimation of the DRE of absorbing aerosols above clouds.

4. Assessing the stability of the retrieval

One of the major benefits from using SEVIRI is the ability to track both aerosol and cloud events at high temporal resolution. Therefore, it is important to evaluate how consistent the retrieval is over time. For that purpose, two days of continuous observations (i.e. 5th and 6th September 2017) have been analysed and the retrieved properties have been averaged over 20˚S and 10˚S, and 5˚E and 15˚E. The above-cloud AOT, COT and CER time series are presented in Figures 12a, b and c. The studied area is located next to the coast, where the AOT is typically the highest. The above-cloud AOT is around 0.66 and 0.72 for the 5th and the 6th September, respectively. As expected, the transport of the aerosol plume from east to west is slow, resulting in a small evolution of the above-cloud AOT that can be expressed as a linear trend. In order to assess the variability of the retrieved AOT, the linear trend +/- 2 times the standard deviation have been plotted on figure 12a (dashed lines). On both days, a peak is observed at 12:15pm with an anomaly larger than the AOT variability. The evolution of the cloud properties is slightly more complex. A small decrease is observed on both the COT and CER until 2pm. After 3pm, both properties sharply increase. The clouds are strongly affected by the diurnal cycle and a shoaling of the cloud cover is expected from early morning to late afternoon. As the thinnest clouds vanish, the cloud fraction decreases together with the number of retrievals in the area. This results in a larger contribution of the thickest clouds to the mean value in the late afternoon. As for the above-cloud AOT, large variations of the CER are observed around noon. At that time, the sun and the satellite are almost aligned and the scattering angle (fig. 12d) reaches values larger than 175˚ which corresponds to the region where the glory phenomenon is typically observed. Several reasons can explain why the retrieval does not perform well in backscattering direction. The first one is the uncertainty in the LUT due to the truncation of the cloud phase function. Although the TMS correction gives good results, biases still remain in the glory aureole (Iwabushi and Suzuki, 2009). Also, the radiances in the glory are more sensitive to the cloud droplet microphysics (Mayer et al., 2004). The assumption on the variance of the droplet size distribution may induce biases in the retrieval. Therefore, the accuracy of the retrieval cannot be guaranteed within the glory aureole and these observations should be discarded. In Figure 12, the timespans corresponding to the MODIS Aqua and Terra overpasses in the region are highlighted in orange. This shows that MODIS measurements are typically performed before and after SEVIRI observes the glory backscattering over the SEAO, usually allowing comparisons between these instruments. Except from the glory backscattering, the stability observed on the retrieved aerosol and cloud properties reinforces the reliability of the algorithm.

5. Conclusion

Recently, progress has been made in the remote sensing field in order to fill the lack of aerosol above cloud observations. Techniques have been developed to retrieve aerosol and cloud properties over the SEAO from passive remote sensing instruments. These algorithms take advantage of the colour-ratio effect (Jethva et al., 2013), which is the spectral contrast produced by the aerosol absorption above clouds. Although OMI (Torres et al., 2012), MODIS (Jethva et al., 2013; Meyer et al., 2015) and POLDER (Peers et al., 2015) already provide useful information about aerosols above clouds, these instruments are on polar orbiting satellites and their low temporal resolutions prevent monitoring the diurnal variation of the cloud cover and of the DRE of aerosols over the SEAO. For the first time, we have applied a similar algorithm to geostationary measurements from the SEVIRI instrument, which has a repeat cycle of 15 minutes. The method consists in a LUT approach, using the channels at 0.64, 0.81 and 1.64 µm in order to retrieve simultaneously the above-cloud AOT, COT and CER.

Compared to other satellite instruments, the SEVIRI measurements are more sensitive to the absorption from atmospheric gases because of the wider spectral bands. Therefore, an efficient atmospheric correction scheme is essential in order to separate the aerosol absorption from the atmospheric gas contribution. Atmospheric transmittances are calculated with the fast-radiative transfer model RTTOV based on the cloud top height observed by SEVIRI and the forecasted water vapour profiles from the Met Office Unified Model. The water vapour correction has the largest impact on the above-cloud aerosol retrieval. The impact of errors in the atmospheric correction has been evaluated by modulating the humidity profile for a case study. A positive bias of both the AOT and the COT is observed when the water vapour is overestimated, and vice versa. On average, an 18.5% bias on the AOT and a 5.5% bias on the COT are expected for a 10% error on the water vapour profile. Although a good accuracy is expected from the forecast model, this limitation should be kept in mind when utilising or further developing SEVIRI products. In the companion paper, the humidity from the forecast will be compared against the dropsonde measurements from the CLARIFY-2017 campaign.

The choice of the aerosol model used to produce the LUT is also a key feature of the method. *In situ* measurements of aerosols above clouds have been performed off the coast of Ascension Island during the CLARIFY-2017 field campaign. An aerosol model optimised for the SEVIRI spectral bands has been obtained by analysing the vertical profiles of extinction and absorption from EXSCALABAR together with the size distribution from a PCASP. A bimodal lognormal distribution has shown to adequately reproduce the observations. A fine mode radius of 0.12 µm has been obtained, which is in good agreement with the biomass burning measured over the SEAO during SAFARI 2000 (Haywood et al., 2003). The refractive index has been evaluated at 1.51-0.029i. The corresponding SSA of 0.85 at 0.55 µm is consistent with both *in situ* and remote sensing observations of African biomass burning aerosols (Johnson et al., 2008; Sayer et al., 2014). In addition to the uncertainty associated with the estimation of the aerosol model, a seasonal dependence is expected in the biomass burning properties as well as modifications due to aging processes during their transport over the SEAO. We have evaluated the impact of applying a single model assumption on both aerosol and cloud properties. Retrievals have been performed considering aerosol models with modified size distributions and refractive indexes. It has been shown that the sensitivity of the retrieved cloud properties to the aerosol model is small with errors lower than 3% on the COT and the CER. As expected the impact of the aerosol model assumption is much larger on the above-cloud AOT, with an uncertainty estimated at 31.2%. Owing to the sensitivity of the method to the aerosol absorption above clouds, a better accuracy is obtained on the retrieved AAOT, with an error of 6.1% only. This indicates that the estimated above-cloud AOT can be easily converted from one aerosol model to another and that the results can be used to estimate the aerosol DRE above clouds.

Despite the wider channels and the narrower spectral range of SEVIRI, it has been demonstrated that the geostationary instrument has the potential to detect and quantify the absorbing aerosol plumes transported above the clouds of the SEAO. Except from observations within the glory backscattering for which the retrieval has shown to be unstable, a good consistency has been observed on the aerosol and cloud properties. The stability of the results during the day is promising for future uses of the SEVIRI algorithm. In the companion paper, the reliability of the retrieved aerosol and cloud properties will be further assessed by analysing the consistency with the MODIS retrievals and comparing with direct measurements from the CLARIFY-2017 field campaign. The potential of such a retrieval is obvious. The 15-minute resolution will aid in tracking the fate of above cloud biomass burning aerosol and will prove invaluable for assessing models of the emission, transport and deposition of biomass burning aerosol, with implications for accurate determination of the direct radiative effects of biomass burning aerosol at high temporal resolution.

Author contribution

FP, PF and JMH developed the concept and the ideas for the conduction of this paper. PF implemented the atmospheric correction scheme and FP, the retrieval algorithm. CF, SJA, KS, MIC, NW and JM operated, calibrated and prepared the *in situ* measurements from EXSCALABAR and the PCASP. The reliability of the retrieved products was analysed throughout the development of the algorithm with the help of KGM and SEP. FP carried out the analysis and prepared the manuscript with contributions from all co-authors.

Acknowledgement

This research was funded by the NERC CLARIFY project NE/L013479/1. Further support was provided by the Research Council of Norway via the projects AC/BC (240372) and NetBC (244141)

References

Aminou, D. M. A., Jacquet, B., and Pasternak, F.: Characteristics of the Meteosat Second Generation (MSG) radiometer/imager: SEVIRI, Proc. SPIE, 3221, 3221 – 3221 – 13, https://doi.org/10.1117/12.298084, 1997.

Brindley, H. and Ignatov, A.: Retrieval of mineral aerosol optical depth and size information from Meteosat Second Generation SEVIRI solar reflectance bands, Remote Sensing of Environment, 102, 344 – 363, https://doi.org/https://doi.org/10.1016/j.rse.2006.02.024, http://www.sciencedirect.com/science/article/pii/S0034425706000952, 2006.

Browell, E. V., Fenn, M. A., Butler, C. F., Grant, W. B., Clayton, M. B., Fishman, J., Bachmeier, A. S., Anderson, B. E., Gregory, G. L., Fuelberg, H. E., Bradshaw, J. D., Sandholm, S. T., Blake, D. R., Heikes, B. G., Sachse, G. W., Singh, H. B., and Talbot, R. W.: Ozone and aerosol distributions and air mass characteristics over the South Atlantic Basin during the burning season, Journal of Geophysical Research: Atmospheres, 101, 24 043–24 068, https://doi.org/10.1029/95JD02536, https://agupubs.onlinelibrary.wiley.com/doi/abs/10.1029/95JD02536, 1996.

Brown, A., Milton, S., Cullen, M., Golding, B., Mitchell, J., and Shelly, A.: Unified Modeling and Prediction of Weather and Climate: A 25-Year Journey, Bulletin of the American Meteorological Society, 93, 1865–1877, https://doi.org/10.1175/BAMS-D-12-00018.1, 2012.

Chang, I. and Christopher, S. A.: Identifying Absorbing Aerosols Above Clouds From the Spinning Enhanced Visible and Infrared Imager Coupled With NASA A-Train Multiple Sensors, IEEE Transactions on Geoscience and Remote Sensing, 54, 3163–3173, https://doi.org/10.1109/TGRS.2015.2513015, 2016.

Clayton, A. M., Lorenc, A. C., and Barker, D. M.: Operational implementation of a hybrid ensemble/4D-Var global data assimilation system at the Met Office, Quarterly Journal of the Royal Meteorological Society, 139, 1445–1461, https://doi.org/10.1002/qj.2054, https://rmets.onlinelibrary.wiley.com/doi/abs/10.1002/qj.2054, 2013.

Davies, N. W., Cotterell, M. I., Fox, C., Szpek, K., Haywood, J. M., and Langridge, J. M.: On the accuracy of aerosol photoacoustic spectrometer calibrations using absorption by ozone, Atmospheric Measurement Techniques, 11, 2313–2324, https://doi.org/10.5194/amt-11-2313-2018, https://www.atmos-meas-tech.net/11/2313/2018/, 2018.

de Graaf, M., Tilstra, L. G., Wang, P., and Stammes, P.: Retrieval of the aerosol direct radiative effect over clouds from spaceborne spectrometry, Journal of Geophysical Research: Atmospheres, 117, https://doi.org/10.1029/2011JD017160, https://agupubs.onlinelibrary.wiley.com/doi/abs/10.1029/2011JD017160, 2012.

de Haan, J. F., Bosma, P., and Hovenier, J.: The adding method for multiple scattering calculations of polarized light, Astronomy and Astrophysics, 183, 371–391, 1987.

Eck, T. F., Holben, B. N., Ward, D. E., Mukelabai, M. M., Dubovik, O., Smirnov, A., Schafer, J. S., Hsu, N. C., Piketh, S. J., Queface, A., Roux, J. L., Swap, R. J., and Slutsker, I.: Variability of biomass burning aerosol optical characteristics in southern Africa during the SAFARI 2000 dry season campaign and a comparison of single scattering albedo estimates from radiometric measurements, Journal of Geophysical Research: Atmospheres, 108, https://doi.org/10.1029/2002JD002321, https://agupubs.onlinelibrary.wiley.com/doi/abs/10.1029/2002JD002321, 2003.

Edwards, J. M. and Slingo, A.: Studies with a flexible new radiation code. I: Choosing a configuration for a large-scale model, Quarterly Journal of the Royal Meteorological Society, 122, 689–719, https://doi.org/10.1002/qj.49712253107, https://rmets.onlinelibrary.wiley.com/doi/abs/10.1002/qj.49712253107, 1996.

Francis, P. N., Hocking, J. A., and Saunders, R. W.: Improved diagnosis of low-level cloud from MSG SEVIRI data for assimilation into Met Office limited area models, in: Proceedings of the 2008 EUMETSAT Meteorological Satellite Conference, Darmstadt, 2008.

Gordon, H., Field, P. R., Abel, S. J., Dalvi, M., Grosvenor, D. P., Hill, A. A., Johnson, B. T., Miltenberger, A. K., Yoshioka, M., and Carslaw, K. S.: Large simulated radiative effects of smoke in the south-east Atlantic, Atmospheric Chemistry and Physics, 18, 15 261– 15 289, https://doi.org/10.5194/acp-18-15261-2018, https://www.atmos-chem-phys.net/18/15261/2018/, 2018.

Hamann, U., Walther, A., Baum, B., Bennartz, R., Bugliaro, L., Derrien, M., Francis, P. N., Heidinger, A., Joro, S., Kniffka, A., Le Gleau, H., Lockhoff, M., Lutz, H. J., Meirink, J. F., Minnis, P., Palikonda, R., Roebeling, R., Thoss, A., Platnick, S., Watts, P., and Wind, G.: Remote sensing of cloud top pressure/height from SEVIRI : analysis of ten current retrieval algorithms, Atmospheric Measurement Techniques, 7, 2839–2867, https://doi.org/10.5194/amt-7-2839-2014, 2014.

Haywood, J. M., Osborne, S. R., Francis, P. N., Keil, A., Formenti, P., Andreae, M. O., and Kaye, P. H.: The mean physical and optical properties of regional haze dominated by biomass burning aerosol measured from the C-130 aircraft during SAFARI 2000, Journal of Geophysical Research: Atmospheres, 108, https://doi.org/10.1029/2002JD002226, https://agupubs.onlinelibrary.wiley.com/doi/abs/10. 1029/2002JD002226, 2003.

Haywood, J. M., Osborne, S. R., and Abel, S. J.: The effect of overlying absorbing aerosol layers on remote sensing retrievals of cloud effective radius and cloud optical depth, Quarterly Journal of the Royal Meteorological Society, 130, 779–800, https://doi.org/10.1256/qj.03.100, https://rmets.onlinelibrary.wiley.com/doi/abs/10.1256/qj.03.100, 2004.

Herman, M., Deuzé, J.-L., Marchand, A., Roger, B., and Lallart, P.: Aerosol remote sensing from POLDER/ADEOS over the ocean: Improved retrieval using a nonspherical particle model, Journal of Geophysical Research: Atmospheres, 110, https://doi.org/10.1029/2004JD004798, https://agupubs.onlinelibrary.wiley.com/doi/abs/10.1029/2004JD004798, 2005.

Hocking, J., Rayer, P., Rundle, D., Saunders, R., Matricardi, M., Geer, A., Brunel, P., and Vidot, J.: RTTOV v11 Users Guide, NWP-SAF Report; Met Office: Exeter, UK, 2014.

Iwabuchi, H. and Suzuki, T.: Fast and accurate radiance calculations using truncation approximation for anisotropic scattering phase functions, Journal of Quantitative Spectroscopy and Radiative Transfer, 110, 1926 – 1939, https://doi.org/https://doi.org/10.1016/j.jqsrt.2009.04.006, http://www.sciencedirect.com/science/article/pii/S0022407309001496, 2009.

Jethva, H., Torres, O., Remer, L. A., and Bhartia, P. K.: A Color Ratio Method for Simultaneous Retrieval of Aerosol and Cloud Optical Thickness of Above-Cloud Absorbing Aerosols From Passive Sensors: Application to MODIS Measurements, IEEE Transactions on Geoscience and Remote Sensing, 51, 3862 – 3870, https://doi.org/10.1109/TGRS.2012.2230008, 2013.

Johnson, B. T., Osborne, S. R., Haywood, J. M., and Harrison, M. A. J.: Aircraft measurements of biomass burning aerosol over West Africa during DABEX, Journal of Geophysical Research: Atmospheres, 113, https://doi.org/10.1029/2007JD009451, https://agupubs. onlinelibrary.wiley.com/doi/abs/10.1029/2007JD009451, 2008.

Keil, A. and Haywood, J. M.: Solar radiative forcing by biomass burning aerosol particles during SAFARI 2000: A case study based on measured aerosol and cloud properties, Journal of Geophysical Research: Atmospheres, 108, https://doi.org/10.1029/2002JD002315, https://agupubs.onlinelibrary.wiley.com/doi/abs/10.1029/2002JD002315, 2003.

Koppmann, R., von Czapiewski, K., and Reid, J. S.: A review of biomass burning emissions, part I: gaseous emissions of carbon monoxide, methane, volatile organic compounds, and nitrogen containing compounds, Atmospheric Chemistry and Physics Discussions, 5, 10 455–10 516, https://doi.org/10.5194/acpd-5-10455-2005, https://www.atmos-chem-phys-discuss.net/5/10455/2005/, 2005.

Koren, I., Kaufman, Y. J., Remer, L. A., and Martins, J. V.: Measurement of the Effect of Amazon Smoke on Inhibition of Cloud Formation, Science, 303, 1342–1345, https://doi.org/10.1126/science.1089424, http://science.sciencemag.org/content/303/5662/1342, 2004.

Levy, R. C., Remer, L. A., Tanre, D., Mattoo, S., and Kaufman, Y. J.: Algorithm for remote sensing of tropospheric aerosol over dark targets from MODIS: Collections 005 and 051: Revision 2; Feb 2009, MODIS algorithm theoretical basis document, 2009.

Lu, Z., Liu, X., Zhang, Z., Zhao, C., Meyer, K., Rajapakshe, C., Wu, C., Yang, Z., and Penner, J. E.: Biomass smoke from southern Africa can significantly enhance the brightness of stratocumulus over the southeastern Atlantic Ocean, Proceedings of the National Academy of Sciences, 115, 2924–2929, https://doi.org/10.1073/pnas.1713703115, https://www.pnas.org/content/115/12/2924, 2018.

Magi, B. I. and Hobbs, P. V.: Effects of humidity on aerosols in southern Africa during the biomass burning season, Journal of Geophysical Research: Atmospheres, 108, https://doi.org/10.1029/2002JD002144, https://agupubs.onlinelibrary.wiley.com/doi/abs/10. 1029/2002JD002144, 2003.

Manners, J.: Socrates technical guide suite of community radiative transfer codes based on edwards and slingo, in: Tech. Rep., Met Office, FitzRoy Rd, Exeter EX1 3PB, 2015.

Matricardi, M.: The generation of RTTOV regression coefficients for IASI and AIRS using a new profile training set and a new line-by-line database, European Centre for Medium-Range Weather Forecasts, 2008.

Matricardi, M., Chevallier, F., Kelly, G., and Thépaut, J.-N.: An improved general fast radiative transfer model for the assimilation of radiance observations, Quarterly Journal of the Royal Meteorological Society, 130, 153–173, https://doi.org/10.1256/qj.02.181, https: //rmets.onlinelibrary.wiley.com/doi/abs/10.1256/qj.02.181, 2004.

Mayer, B., Schröder, M., Preusker, R., and Schüller, L.: Remote sensing of water cloud droplet size distributions using the backscatter glory: a case study, Atmospheric Chemistry and Physics, 4, 1255–1263, https://doi.org/10.5194/acp-4-1255-2004, https://www. atmos-chem-phys.net/4/1255/2004/, 2004.

McClatchey, R. A., Fenn, R. W., Selby, J. A., Volz, F., and Garing, J.: Optical properties of the atmosphere, Tech. rep., Air Force Cambridge Research Labs Hanscom AFB MA, 1972.

Atmos. Chem. Phys. Discuss., https://doi.org/10.5194/acp-2018-1333
Manuscript under review for journal Atmos. Chem. Phys.
Discussion started: 10 January 2019

Meyer, K., Platnick, S., and Zhang, Z.: Simultaneously inferring above-cloud absorbing aerosol optical thickness and underlying liquid phase cloud optical and microphysical properties using MODIS, Journal of Geophysical Research: Atmospheres, 120, 5524–5547, https://doi.org/10.1002/2015JD023128, https://agupubs.onlinelibrary.wiley.com/doi/abs/10.1002/2015JD023128, 2015.

Min, M. and Zhang, Z.: On the influence of cloud fraction diurnal cycle and sub-grid cloud optical thickness variability on all-sky direct aerosol radiative forcing, Journal of Quantitative Spectroscopy and Radiative Transfer, 142, 25 – 36, https://doi.org/https://doi.org/10.1016/j.jqsrt.2014.03.014, http://www.sciencedirect.com/science/article/pii/S0022407314001307, 2014.

Nakajima, T. and King, M. D.: Determination of the Optical Thickness and Effective Particle Radius of Clouds from Reflected Solar Radiation Measurements. Part I: Theory, Journal of the Atmospheric Sciences, 47, 1878–1893, https://doi.org/10.1175/1520-0469(1990)047<1878:DOTOTA>2.0.CO;2, 1990.

Nakajima, T. and Tanaka, M.: Algorithms for radiative intensity calculations in moderately thick atmospheres using a truncation approximation, Journal of Quantitative Spectroscopy and Radiative Transfer, 40, 51 – 69, https://doi.org/https://doi.org/10.1016/0022-4073(88)90031-3, http://www.sciencedirect.com/science/article/pii/0022407388900313, 1988.

Peers, F., Waquet, F., Cornet, C., Dubuisson, P., Ducos, F., Goloub, P., Szczap, F., Tanré, D., and Thieuleux, F.: Absorption of aerosols above clouds from POLDER/PARASOL measurements and estimation of their direct radiative effect, Atmospheric Chemistry and Physics, 15, 4179–4196, https://doi.org/10.5194/acp-15-4179-2015, https://www.atmos-chem-phys.net/15/4179/2015/, 2015.

Peers, F., Bellouin, N., Waquet, F., Ducos, F., Goloub, P., Mollard, J., Myhre, G., Skeie, R. B., Takemura, T., Tanré, D., Thieuleux, F., and Zhang, K.: Comparison of aerosol optical properties above clouds between POLDER and AeroCom models over the South East Atlantic Ocean during the fire season, Geophysical Research Letters, 43, 3991–4000, https://doi.org/10.1002/2016GL068222, https://agupubs.onlinelibrary.wiley.com/doi/abs/10.1002/2016GL068222, 2016.

Platnick, S., Ackerman, S., King, M., Meyer, K., Menzel, W., Holz, R., Baum, B., and Yang, P.: MODIS atmosphere L2 cloud product (06_L2), NASA MODIS Adaptive Processing System, Goddard Space Flight Center, 2015.

Rosenberg, P. D., Dean, A. R., Williams, P. I., Dorsey, J. R., Minikin, A., Pickering, M. A., and Petzold, A.: Particle sizing calibration with refractive index correction for light scattering optical particle counters and impacts upon PCASP and CDP data collected during the Fennec campaign, Atmospheric Measurement Techniques, 5, 1147–1163, https://doi.org/10.5194/amt-5-1147-2012, https://www. atmos-meas-tech.net/5/1147/2012/, 2012.

Rosenfeld, D.: Suppression of Rain and Snow by Urban and Industrial Air Pollution, Science, 287, 1793–1796, https://doi.org/10.1126/science.287.5459.1793, http://science.sciencemag.org/content/287/5459/1793, 2000.

Sayer, A. M., Hsu, N. C., Eck, T. F., Smirnov, A., and Holben, B. N.: AERONET-based models of smoke-dominated aerosol near source regions and transported over oceans, and implications for satellite retrievals of aerosol optical depth, Atmospheric Chemistry and

Physics, 14, 11 493–11 523, https://doi.org/10.5194/acp-14-11493-2014, https://www.atmos-chem-phys.net/14/11493/2014/, 2014.

Thieuleux, F., Moulin, C., Bréon, F. M., Maignan, F., Poitou, J., and Tanré, D.: Remote sensing of aerosols over the oceans using MSG/SEVIRI imagery, Annales Geophysicae, 23, 3561–3568, https://doi.org/10.5194/angeo-23-3561-2005, 2005.

Torres, O., Jethva, H., and Bhartia, P. K.: Retrieval of Aerosol Optical Depth above Clouds from OMI Observations: Sensitivity Analysis and Case Studies, Journal of the Atmospheric Sciences, 69, 1037–1053, https://doi.org/10.1175/JAS-D-11-0130.1, 2012.

Twomey, S.: Pollution and the planetary albedo, Atmospheric Environment (1967), 8, 1251 – 1256, https://doi.org/10.1016/0004-6981(74)90004-3, http://www.sciencedirect.com/science/article/pii/0004698174900043, 1974.

Waquet, F., Cornet, C., Deuzé, J.-L., Dubovik, O., Ducos, F., Goloub, P., Herman, M., Lapyonok, T., Labonnote, L. C., Riedi, J., Tanré, D., Thieuleux, F., and Vanbauce, C.: Retrieval of aerosol microphysical and optical properties above liquid clouds from POLDER/PARASOL polarization measurements, Atmospheric Measurement Techniques, 6, 991–1016, https://doi.org/10.5194/amt- 6-991-2013, https://www.atmos-meas-tech.net/6/991/2013/, 2013a.

Waquet, F., Peers, F., Ducos, F., Goloub, P., Platnick, S., Riedi, J., Tanré, D., and Thieuleux, F.: Global analysis of aerosol properties above clouds, Geophysical Research Letters, 40, 5809–5814, https://doi.org/10.1002/2013GL057482, https://agupubs.onlinelibrary.wiley.com/doi/abs/10.1002/2013GL057482, 2013b.

Watts, P., Mutlow, C., Baran, A., and Zavody, A.: Study on cloud properties derived from Meteosat Second Generation observations, EUMETSAT ITT, 97, 181, 1998.

Wilcox, E. M.: Stratocumulus cloud thickening beneath layers of absorbing smoke aerosol, Atmospheric Chemistry and Physics, 10, 11 769–11 777, https://doi.org/10.5194/acp-10-11769-2010, https://www.atmos-chem-phys.net/10/11769/2010/, 2010.

Wilcox, E. M.: Direct and semi-direct radiative forcing of smoke aerosols over clouds, Atmospheric Chemistry and Physics, 12, 139–149, https://doi.org/10.5194/acp-12-139-2012, https://www.atmos-chem-phys.net/12/139/2012/, 2012.

Wiscombe, W.: The Delta–M method: Rapid yet accurate radiative flux calculations for strongly asymmetric phase functions, Journal of the atmospheric sciences, 34, 1408–1422, 1977.

Zuidema, P., Redemann, J., Haywood, J., Wood, R., Piketh, S., Hipondoka, M., and Formenti, P.: Smoke and Clouds above the Southeast Atlantic: Upcoming Field Campaigns Probe Absorbing Aerosol's Impact on Climate, Bulletin of the American Meteorological Society, 97, 1131–1135, https://doi.org/10.1175/BAMS-D-15-00082.1, 2016.

Zuidema, P., Sedlacek III, A. J., Flynn, C., Springston, S., Delgadillo, R., Zhang, J., Aiken, A. C., Koontz, A., and Muradyan, P.: The Ascension Island Boundary Layer in the Remote Southeast Atlantic is Often Smoky, Geophysical Research Letters, 45, 4456–4465, https://doi.org/10.1002/2017GL076926, https://agupubs.onlinelibrary.wiley.com/doi/abs/10.1002/2017GL076926, 2018.

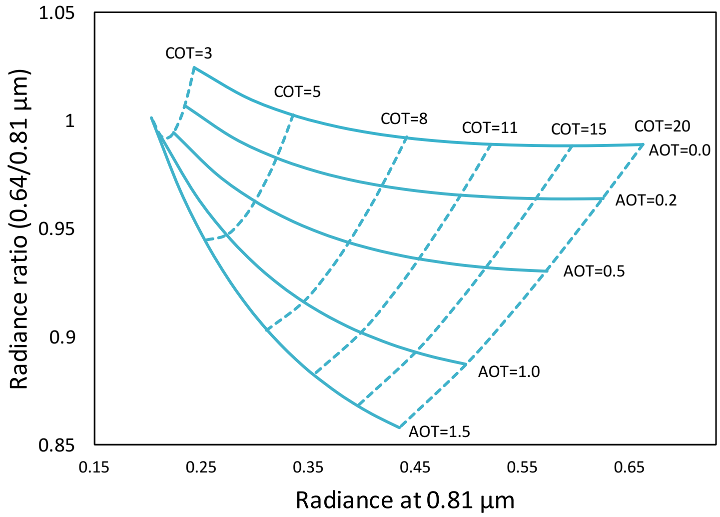

Figure 1: Radiance ratio $R_{0.64}/R_{0.81}$ as a function of the radiance at 0.81µm for absorbing aerosols above clouds simulated with the adding-doubling method (De Haan et al., 1987). Cloud optical thicknesses (COT) and aerosol optical thicknesses (AOT) are indicated at 0.55 µm.

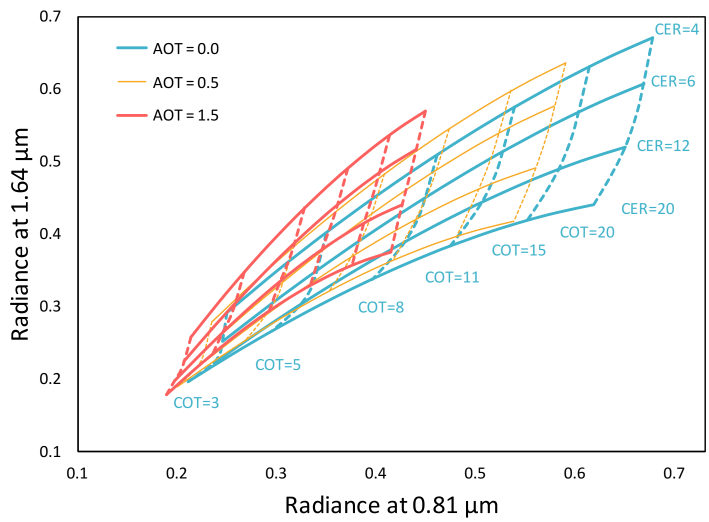

Figure 2: Simulated radiances at 1.64 and 0.81µm for clouds with varying COT and CER (in µm), without (blue) and with (orange and red) absorbing aerosols above. The viewing geometry, the aerosol and the cloud properties are the same as Figure 1.

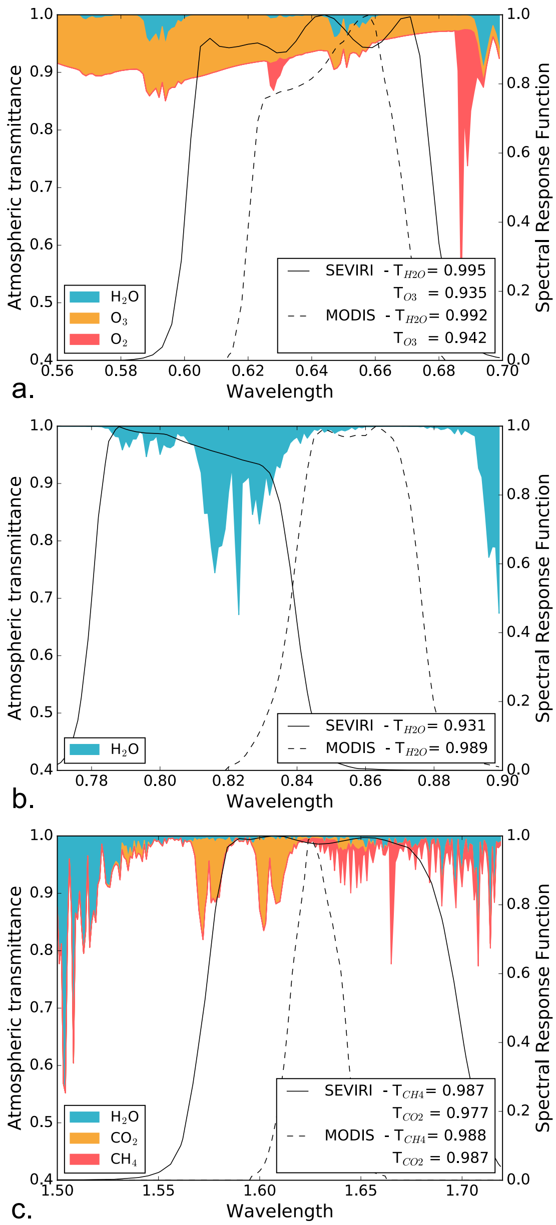

Figure 3: Spectral response function of the SEVIRI bands at 0.64 (a), 0.81 (b) and 1.64 µm (c) with the corresponding MODIS ones (dashed lines) as well as the atmospheric transmittance within the spectral range (in colour). The transmittances have been calculated with the SOCRATES radiative transfer scheme (Manners et al., 2015; Edwards and Slingo, 1996) assuming a humidity profile measured during SAFARI (Keil and Haywood, 2003). In the legend of each plot, the transmittance weighted by the spectral response function is given for the main absorbing gases.

Atmos. Chem. Phys. Discuss., https://doi.org/10.5194/acp-2018-1333
Manuscript under review for journal Atmos. Chem. Phys.
Discussion started: 10 January 2019

Atmospheric Chemistry and Physics Discussions
Open Access

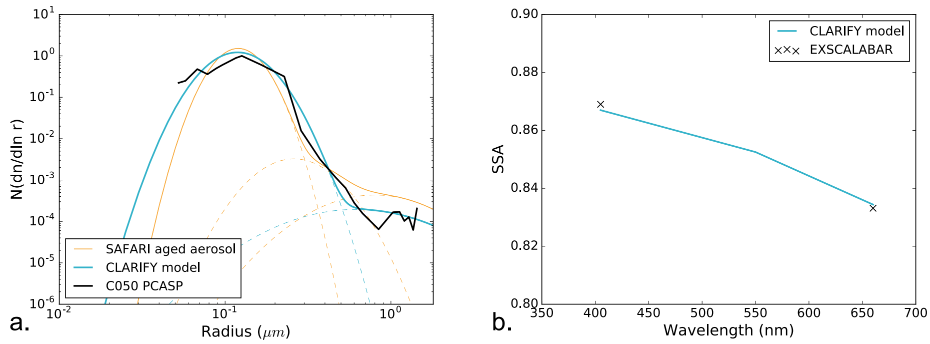

Figure 4: Normalized size distribution (a) and SSA (b) measured above clouds during flight C050 of the CLARIFY-2017 campaign (black). Blue lines represent the fitted aerosol model, the orange ones correspond to the aged aerosol size distribution from SAFARI (Haywood et al., 2003), and the dashed lines shows the contribution of each mode. CLARIFY-2017 aerosol model: [r_{fine}, σ_{fine}, N_{fine}; r_{coarse}, σ_{coarse}, N_{coarse}] = [0.12µm, 1.42, 0.963; 0.62µm, 2.23, 0.037], refractive index = 1.51 – 0.029i. SAFARI aged aerosol model: [r_1, σ_1, N_1; r_2, σ_2, N_2; r_3, σ_3, N_3] = [0.12µm, 1.30, 0.996; 0.26µm, 1.50, 0.0033; 0.80µm, 1.90, 0.0007].

		Aerosol model		
Size distribution		Bimodal lognormal distribution		
	r_{fine} = 0.12 µm	σ_{fine} = 1.42		N_{fine} = 0.963
	r_{coarse} = 0.62 µm	σ_{coarse} = 2.23		N_{coarse} = 0.037
Refractive index		1.51 – 0.029i		
Wavelength	0.55 µm*	0.64 µm	0.81 µm	1.64 µm
SSA	0.852	0.839	0.804	0.643
g	0.649	0.612	0.538	0.468
		Cloud model		
Size distribution		Gamma law		
	r_{eff} from 4 to 60 µm		v_{eff} = 0.06	

Table 1: Aerosol and cloud properties used to compute the radiances LUT of the SEVIRI retrieval. (* Note that 0.55µm does not correspond to a SEVIRI channel.)

Atmos. Chem. Phys. Discuss., https://doi.org/10.5194/acp-2018-1333
Manuscript under review for journal Atmos. Chem. Phys.
Discussion started: 10 January 2019

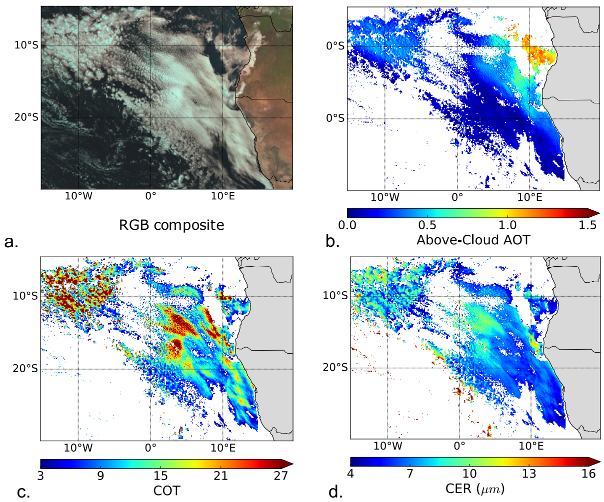

Figure 5: RGB composite (a), Above cloud AOT at 550 nm (b) and cloud properties (c and d) retrieved from SEVIRI measurements on the 28 August 2017 at 10:12 UTC over the SEAO.

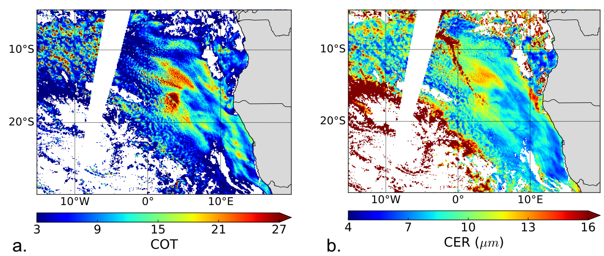

Figure 6: Cloud Optical Thickness (COT) and droplet effective radius (CER) from the MODIS-Terra Collection 6 for the 28 August 2017 (Platnick et al., 2015).

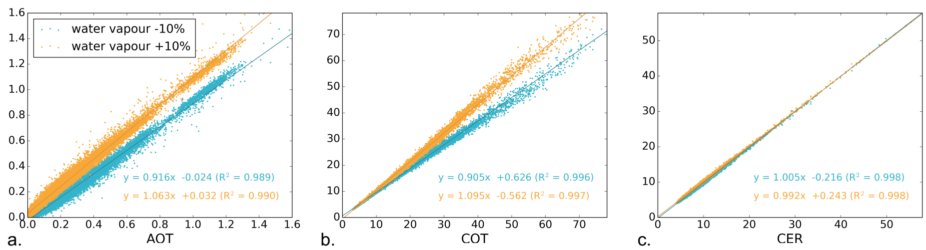

Figure 7: Uncertainty in the retrieved above-cloud AOT (a), COT (b) and CER(c) due to an error of +10% in orange and -10% in blue on the water vapour profile compare to the original forecast for the 28 August 2017 at 10:12 UTC.

Atmos. Chem. Phys. Discuss., https://doi.org/10.5194/acp-2018-1333
Manuscript under review for journal Atmos. Chem. Phys.
Discussion started: 10 January 2019

	Modified parameter	SSA (550 nm)	ΔAOT (%)	ΔAAOT (%)	ΔCOT (%)	ΔCER (%)
Size distribution	$r_{fine,CLARIFY}$ -0.01µm	0.842	-4.9	1.4	-0.2	0.6
	$r_{fine,CLARIFY}$ +0.01µm	0.860	5.8	0.2	0.6	0.6
	σ_{fine}-0.1	0.839	-11.8	-4.0	-1.9	-1.2
	σ_{fine}+0.1	0.859	10.7	5.4	2.5	0.9
Refractive index n	$n_{real,CLARIFY}$-0.02	0.846	-3.4	0.3	-0.3	-0.1
	$n_{real,CLARIFY}$+0.02	0.858	3.4	-0.8	0.3	0.1
	$n_{im,CLARIFY}$-0.008	0.886	38.7	6.5	-0.2	0.3
	$n_{im,CLARIFY}$+0.008	0.822	-17.9	-1.1	0.2	-0.1

Table 2: Aerosol properties used to test the sensitivity of the SEVIRI retrieval and the corresponding differences Δ obtained on the above-cloud AOT, AAOT, COT and CER with respect to retrieved values using the unperturbed aerosol model.

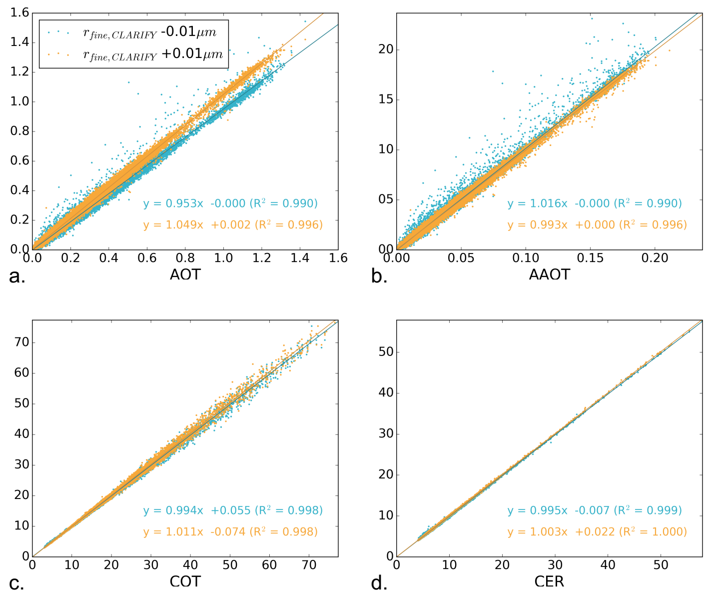

Figure 8: Impact of the assumption on the fine mode radius r_{fine} on the retrieved aerosol and cloud properties. AOT, AAOT, COT and CER obtained for the 28 August 2017 at 10:12 UTC with the modified aerosol models are plotted against the properties retrieved with the CLARIFY-2017 model.

Atmos. Chem. Phys. Discuss., https://doi.org/10.5194/acp-2018-1333
Manuscript under review for journal Atmos. Chem. Phys.
Discussion started: 10 January 2019

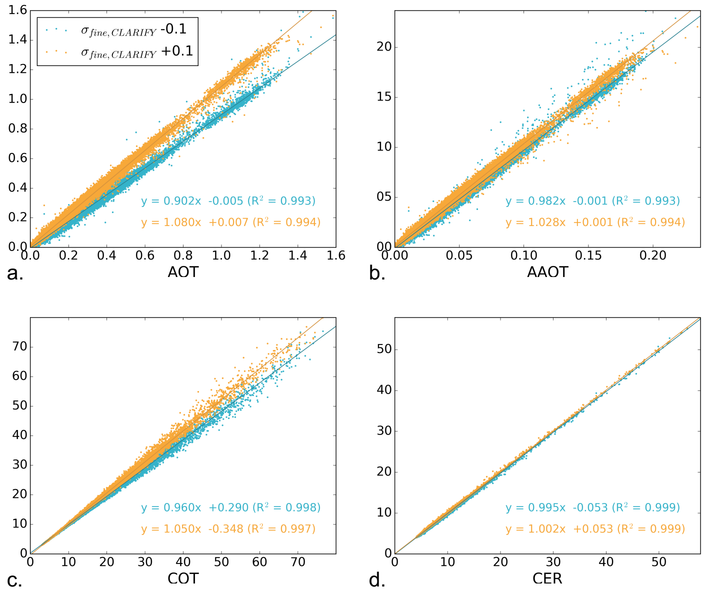

Figure 9: Similar to Figure 8 for the impact of the assumption on the fine mode standard deviation σ_{fine}.

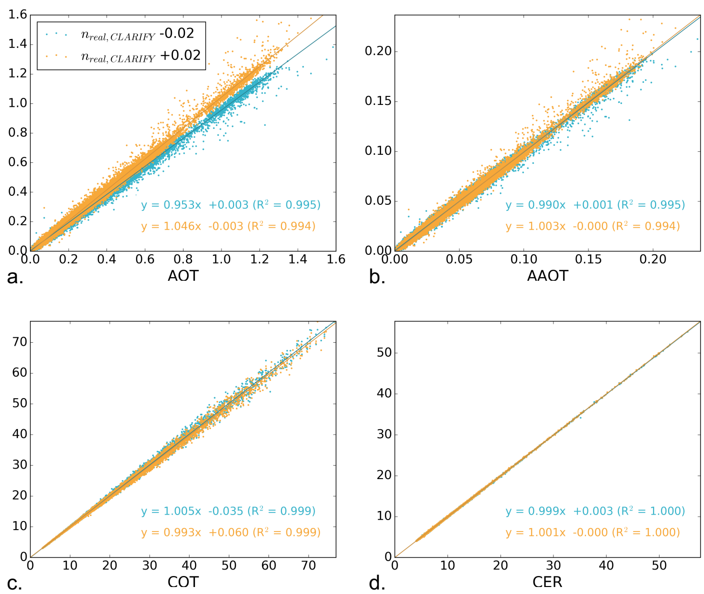

Figure 10: Similar to Figure 8 for the impact of the assumption on the real part of the aerosol refractive index n_{real}.

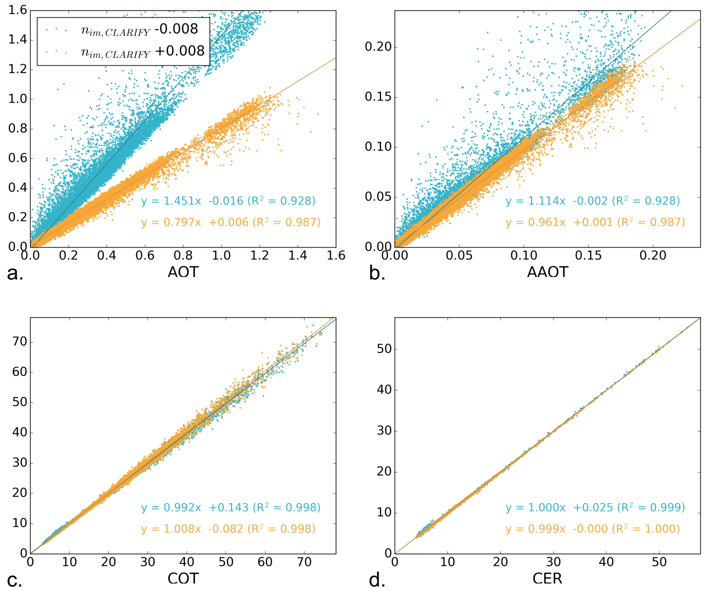

Figure 11: Similar to Figure 8 for the impact of the assumption on the aerosol imaginary part of the refractive index n_{im}.

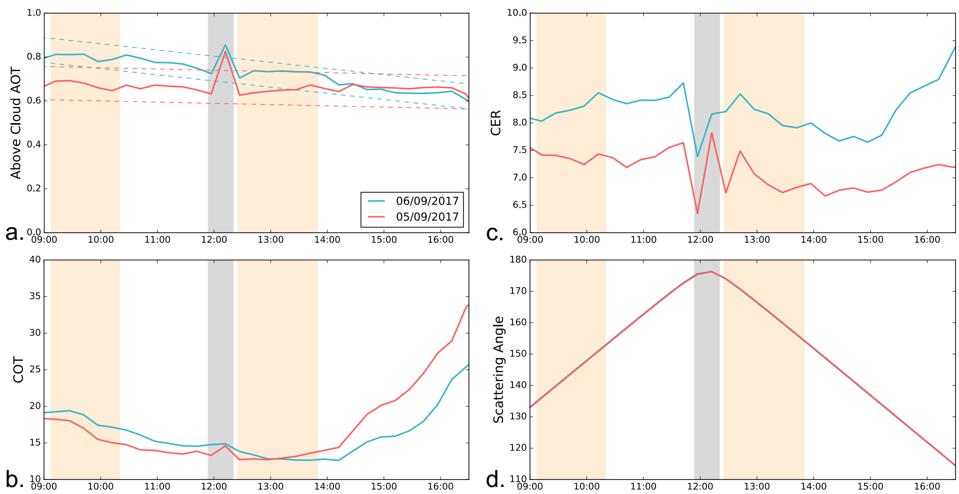

Figure 12: Time series of the above-cloud AOT (a), COT (b), CER(c) and scattering angle(d) averaged between 20˚S and 10˚S, and 5˚E and 15˚E for the 5th and 6th September 2017. The grey area represents scattering angles larger than 175˚ and the orange ones show the typical overpass times of MODIS Aqua and Terra over the region. The dashed lines in figure a corresponds to +/- 2 times the standard deviation.